Journal of
Applied Crystallography

ISSN 0021-8898

Received 9 May 2003
Accepted 22 January 2004

Imaging modulated reflections from a semi-crystalline state of profilin:actin crystals

J. J. Lovelace,[a] K. Narayan,[b] J. K. Chik,[c] H. D. Bellamy,[d]‡ E. H. Snell,[e] U. Lindberg,[f] C. E. Schutt[b] and G. E. O. Borgstahl[a]*

[a]Eppley Institute for Cancer Research, 987696 Nebraska Medical Center, Omaha, NE 68198-7696, USA, [b]Department of Chemistry, Princeton University, Princeton, NJ 08544, USA, [c]Department of Biochemistry and Molecular Biology, Faculty of Medicine, University of Calgary, Calgary, Alberta, T2N 4N1, Canada, [d]Stanford Synchrotron Radiation Laboratory, Menlo Park, CA 94025, USA, [e]NASA Laboratory for Structural Biology, Code SD46, Marshall Space Flight Center, Huntsville, AL 35812, USA, and [f]Department of Zoological Cell Biology, Stockholm University, S-10691 Stockholm, Sweden. Correspondence e-mail: gborgstahl@unmc.edu

Modulated protein crystals remain *terra incognita* for most crystallographers. While small-molecule crystallographers have successfully wrestled with and conquered this type of structure determination, to date no modulated macromolecular structures have been reported. Profilin:β-actin in a modulated semi-crystalline state presents a challenge of sufficient biological significance to motivate the development of methods for the accurate collection of data on the complex diffraction pattern and, ultimately, the solution of its structure. In the present work, fine φ-sliced data collection was used to resolve the closely spaced satellite reflections from these polymorphic crystals. Image-processing methods were used to visualize these data for comparison with the original precession data. These preliminary data demonstrate the feasibility of using fine φ-slicing to collect accurately the intensities and positions of the main and satellite reflections from these modulated protein crystals.

1. Introduction

In an ideal periodic crystal, the contents of the asymmetric unit are perfectly replicated by the symmetry operators of the space group. Inevitable 'real-world' disorder results in departures from this ideality. One particularly fascinating deviation from ideality results in the appearance of distinct satellite reflections around the main Bragg reflections. These satellite reflections are often as sharp as the main spots and result from a structural modulation contained in aperiodic crystals. These modulated structures contain a harmonic variation which destroys the short-range translational symmetry. The term 'aperiodic' includes both positionally and occupationally modulated crystals and composite crystals (Dehling, 1927; Korekawa & Jagodzinski, 1967). The modulation can be incommensurate or commensurate with the main lattice. For the commensurate case, the modulation is a special type of superlattice, and the distortion is smoothly varying and can be described by some harmonic function with an integer-multiple relationship to the main lattice. For the incommensurate case, the relationship with the main lattice is nonintegral. Structural analysis of modulated crystals is based on the theoretical works of de Wolff, Janner and Janssen (Janssen *et al.*, 1999). Today, modulated small-molecule crystals are frequently observed and can be solved; see Daniels *et al.* (2002), Duncan *et al.* (2002) and Gaillard *et al.* (1998) for recent examples. For macromolecular crystals, satellite reflections have only rarely been reported (Pickersgill, 1987; Skrzypczak-Jankun *et al.*, 1996) and, to our knowledge, no modulated macromolecular structures have been solved.

An interesting case of an apparently modulated protein crystal is given by the semi-crystalline diffraction pattern obtained by lowering the pH of the bathing solution of profilin:actin crystals (Schutt *et al.*, 1989). The actin molecules in profilin:actin crystals are organized into ribbon-like filaments *via* intermolecular contacts, forming the crystal lattice (Chik *et al.*, 1996; Schutt *et al.*, 1993). The pH-induced partial dissociation of profilin from actin is thought to result in an in-crystal ribbon-to-helix transition of the actin molecule (Schutt *et al.*, 1997, 1995). There is very little structural data on how actin filaments assemble to test this and other models of the actin filament (see dos Remedios *et al.*, 2003, for a recent review). Thus, the structure determination of profilin:actin in its semi-crystalline state would contribute to our understanding of the actin filament, its dynamic nature, and whether the actin ribbon represents a structural intermediate of the actin filament or not. To date, there have been no structural studies of modulated macromolecular crystals. The biological importance of these challenging modulated crystals of profilin:actin has motivated the development of methods to analyze them in greater detail, with the goal of obtaining a structural explanation of the modulation. The first steps toward such a structural study, *i.e.* the development of data-collection methods to record accurately the positions and intensities of the main and satellite reflections, are presented here.

2. Growth of profilin:actin crystals and transfer to the semi-crystalline state

The following protocol was used to grow crystals of profilin:β-actin at pH 7.3 (Chik *et al.*, 1996) and then transfer these crystals to a semi-crystalline state at pH 6.0 (Chik, 1996; Schutt *et al.*, 1989). Profilin:β-

‡ Present address: Center for Advanced Microstructures and Devices, Louisiana State University, 6980 Jefferson Highway, Baton Rouge, LA 70806, USA.

actin from bovine calf thymus was purified as previously described (Rozycki *et al.*, 1991). The protein was precipitated using ammonium sulfate and then resolubilized at 10–15 mg ml^{-1} in a 5 m*M* potassium phosphate buffer (pH 7.6) containing 0.5 m*M* adenosine-5′-triphosphate (ATP), 0.2 m*M* $CaCl_2$ and 0.5 m*M* dithiothreitol (DTT), and then clarified by ultracentrifugation. The resolubilized protein was then dialyzed into 1.3 *M* potassium phosphate (pH 7.3) containing 0.5 m*M* ATP, 0.2 m*M* $CaCl_2$ and 0.5 m*M* DTT, for batch crystallization at 277 K. Actin paracrystals (a microcrystalline precipitate which competes with growing profilin:actin crystals) were formed, and after 8 h these were removed by ultracentrifugation. At this point, the supernatant contains an excess of free profilin, which promotes the association of profilin:actin into crystals in preference to the formation of actin filaments. There is also an overabundance of crystal nuclei. For crystallization, 5–30 µl drops were suspended above 1 ml of dialysis buffer in the reservoir. In order to obtain large crystals, microcrystals grown in unfiltered hanging drops were used to seed drops filtered with 0.22 µm Millex-GV filter units from Millipore. Crystals grew in 24 to 36 h, to an average size of 0.35 × 0.25 × 0.15 mm. They were then transferred to a stabilizing solution consisting of 1.8 *M* phosphate buffer (pH 7.3) containing 0.5 m*M* ATP and 0.5 m*M* DTT, followed by slow transfer to room temperature. The semi-crystalline state was achieved by transferring the crystals into a buffered solution containing 1.8 *M* potassium phosphate (pH 6.0), 50 µ*M* EGTA [ethyleneglycol-bis(2-aminoethyl-ether)-*N*,*N*,*N*′,*N*′-tetraacetic acid], 4 m*M* $MgCl_2$, 0.5 m*M* ATP and 0.5 m*M* DTT. The transition of the open state to this semi-crystalline state was reproducible.

3. Precession photos of the open and semi-crystalline states of profilin:actin

The semi-crystalline state of profilin:actin was first observed over a decade ago using the precession method (Chik, 1996; Schutt *et al.*, 1989). In Fig. 1, select regions from precession images of profilin:actin crystals in the open state and in the semi-crystalline state are presented. In the 0*kl* plane (Figs. 1*a* and 1*b*), satellite reflections appear along the *k* direction throughout, with a spacing that is about $\frac{1}{3}$ of the normal lattice spacing. The white boxes in Figs. 1(*a*) and 1(*b*) highlight this change. Significant intensity changes are also visible. In the *h*0*l* plane (Figs. 1*c* and 1*d*), the spots seem to split along the *l* direction throughout in the semi-crystalline state.

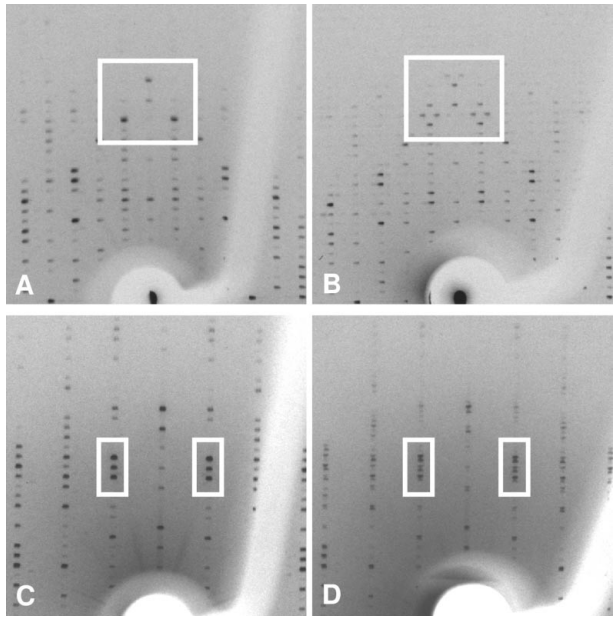

Figure 1
Precession images taken on two planes in the open state and semi-crystalline state for profilin:actin. (*a*) 0*kl* in the open state. (*b*) 0*kl* in the semi-crystalline state. For parts (*a*) and (*b*), *k* is horizontal and *l* is vertical. (*c*) *h*0*l* in the open state. (*d*) *h*0*l* in the semi-crystalline state. For parts (*c*) and (*d*), *h* is horizontal and *l* is vertical. For the semi-crystalline state (comparing *a* with *b*), satellite reflections appear along the *k* direction with a spacing of about $\frac{1}{3}$ of the open-state distance. Also, the semi-crystalline-state reflections become split in the *l* direction (comparing *c* with *d*) and the spacing is approximately $\frac{1}{4}$ to $\frac{1}{5}$ of the open-state distance. For the open state, the space group is $P2_12_12_1$ with unit-cell dimensions $a = 38.14$, $b = 72.45$ and $c = 185.7$ Å (Chik, 1996). For these photographs, the precession angle was 12°, the crystal-to-film distance was 100.0 mm and the exposure time was 12–18 h, using an Elliott *GX*-6 rotating-anode X-ray source.

4. Results from finely sliced rotation geometry synchrotron data collection

The closely spaced modulated diffraction pattern produced by semi-crystalline profilin:actin crystals was measured at Stanford Synchrotron Radiation Laboratory beamline 1-5, using standard rotation geometry and unusually fine φ-slicing (Bellamy *et al.*, 2000). For profilin:actin crystals, a focused beam was used to measure the reflection profiles, as they exhibit weaker diffraction than the manganese superoxide dismutase (MnSOD), insulin and lysozyme crystals previously studied using this method but with a parallel beam (Bellamy *et al.*, 2000; Borgstahl *et al.*, 2001; Snell *et al.*, 2001). The focused beam has significant beam divergence, which broadens the reflection profiles. Consequently, fine slicing steps of 0.010° were used, rather than the 0.001° used in the MnSOD, insulin and lysozyme cases. The beam retained the spectral characteristics given by Bellamy *et al.* (2000), as the focusing mirror is after the monochromator. Data were collected using an ADSC Quantum4 CCD detector. A single semi-crystalline-state crystal with no visible surface cracks was mounted in an X-ray capillary for data collection. The crystal was maintained at 295 K using an FTS system. For the purposes of autoindexing, ten 0.5° 'coarse' oscillation images were taken with an exposure time of 150 s. Reflection profiles over the same oscillation range were then accumulated, with 500 fine sliced still images taken with a separation of 0.010° in φ, each with an exposure time of 40 s. The crystal-to-detector distance was 170 mm and the X-ray wavelength was 1.542 Å (8041 eV). The data were processed using *BEAM-ish* 2.0 software and the intensity profiles were analyzed for any interesting features (Lovelace & Borgstahl, 2003).

All reflection profiles were bimodal. Eight reflections in two vertical sectors on the detector, which had two well separated domains, were selected for further analysis (Fig. 2). Reflections in the other two vertical sectors were also bimodal, but the second part was relatively weak and looked like a sloping shoulder to the left-hand side of the profile (Fig. 2, insets). Reflections in the horizontal sectors were broadened by the beam divergence and the Lorentz effect and could not be separated. The bimodal reflection profiles could indicate either splitting or satellite reflections, as were seen in the precession images. Animations of the reflection topographs along φ were studied using the tools in *BEAM-ish* 2.0 and supported these observations (data not shown). It was difficult to compare the rotation data directly with the precession data, so it was decided to generate a three-dimensional representation of the fine sliced data for the eight reflections in reciprocal space, *hkl* (Fig. 3). The basic mathematics used to produce the three-dimensional representations was described previously (Busing & Levy, 1967; Powell, 1999; Wonacott, 1977), and

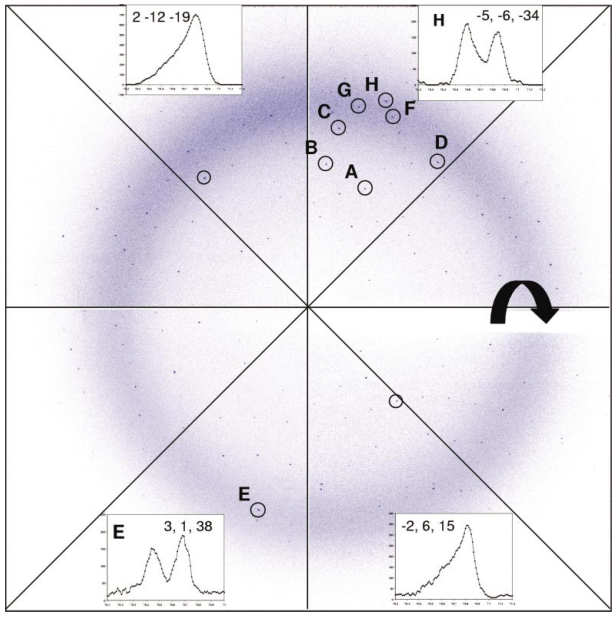

Figure 2
Coarse diffraction data from a 0.5° oscillation of the semi-crystalline state of profilin:actin. The eight highlighted reflections (labelled A–H) were selected for further evaluation with fine slicing. Fine sliced images were collected every 0.010°. The unit cell calculated from the coarse images was a = 38.6, b = 71.6 and c = 174.9 Å. Black lines divide the detector face into sectors and the curved arrow indicates the horizontal rotation axis. The insets show representative reflection profiles (intensity *versus* φ in degrees) from the vertical sectors of the detector, their label (E or H) as appropriate and their hkl values.

was demonstrated elsewhere, using similar data derived from *MOSFLM*, by Vahedi-Faridi and coworkers (Vahedi-Faridi *et al.*, 2003). For each three-dimensional reflection in reciprocal space (Fig. 4), there appear to be two spots which are split roughly down the l axis. This is similar to the data in Figs. 1(*c*) and 1(*d*), which show a split along the l axis for the $h0l$ plane. It is unknown how this splitting manifests itself in other planes. It is interesting that, for a given split reflection, neither of the split spots lies exactly on the assigned index. This is not surprising, since the crystal was indexed using the 0.5° coarse oscillation images (Lovelace *et al.*, 2000). Thus, the x,y location of the reflections on the coarse images was well predicted but the third dimension, along φ, was less accurately defined.

5. Conclusions

The application of fine φ-sliced rotation data collection to a modulated macromolecular crystal for structure determination is promising. A semi-crystalline state of profilin:actin, which may capture the transition state from an extended ribbon form of actin to a ground-state helical form of filamentous actin, has been studied using this method. The direction and approximate spacing of the split reflections collected using this method (Fig. 4) match those observed in the original precession photographs (Fig. 1). Unfortunately, the exact same reflections from the $h0l$ or $0kl$ planes were not measured, so a precise comparison is not possible with these data. The fine sliced reflections most closely match the splitting seen throughout the $h0l$ plane (Fig. 1*d*). There is no evidence in these limited data for the

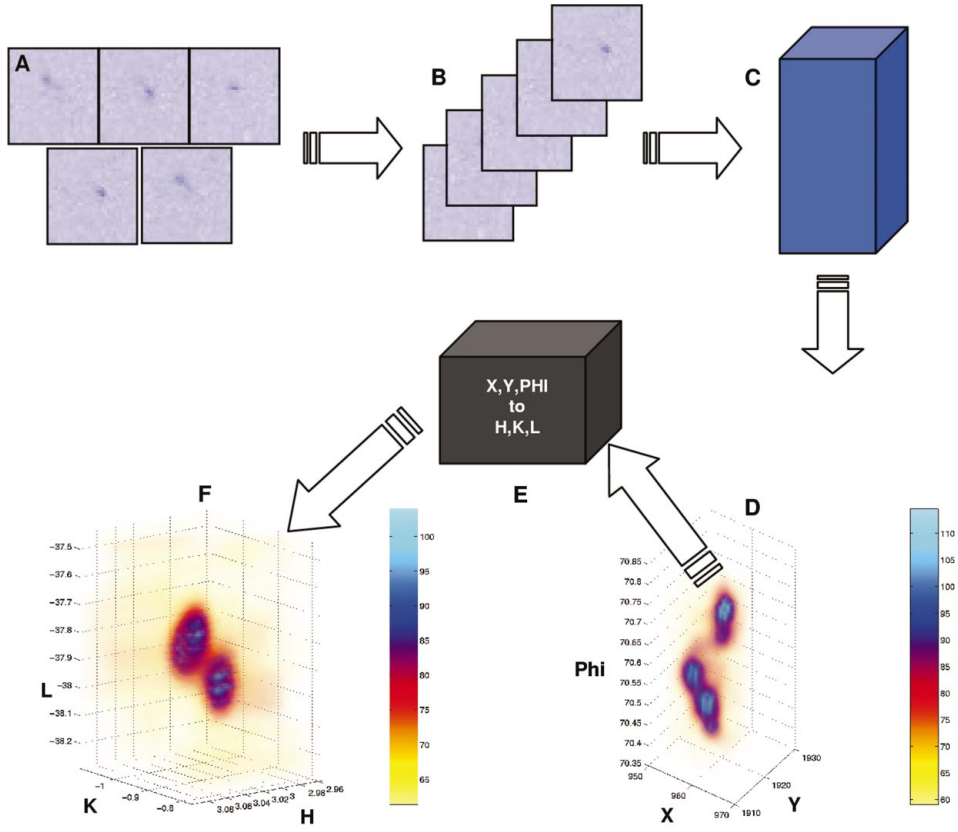

Figure 3
The processing of the fine sliced reflection data in order to display it in reciprocal space and to facilitate comparisons with the precession imagery. (*a*) Sub-images are selected which contain the reflection in the fine sliced data. (*b*) The images are stacked by oscillation range. (*c*) The image stack is converted into a three-dimensional voxel representation, where each voxel is defined by an x pixel location, a y pixel location and the oscillation angle. (*d*) A three-dimensional representation of the data after conversion to voxels. (*e*) The x, y and φ coordinates of each voxel are transformed into reciprocal-lattice coordinates h, k and l. (*e*) The three-dimensional representation of the reflection in reciprocal space. The mathematics in step (*e*) is described by Vahedi-Faridi *et al.* (2003).

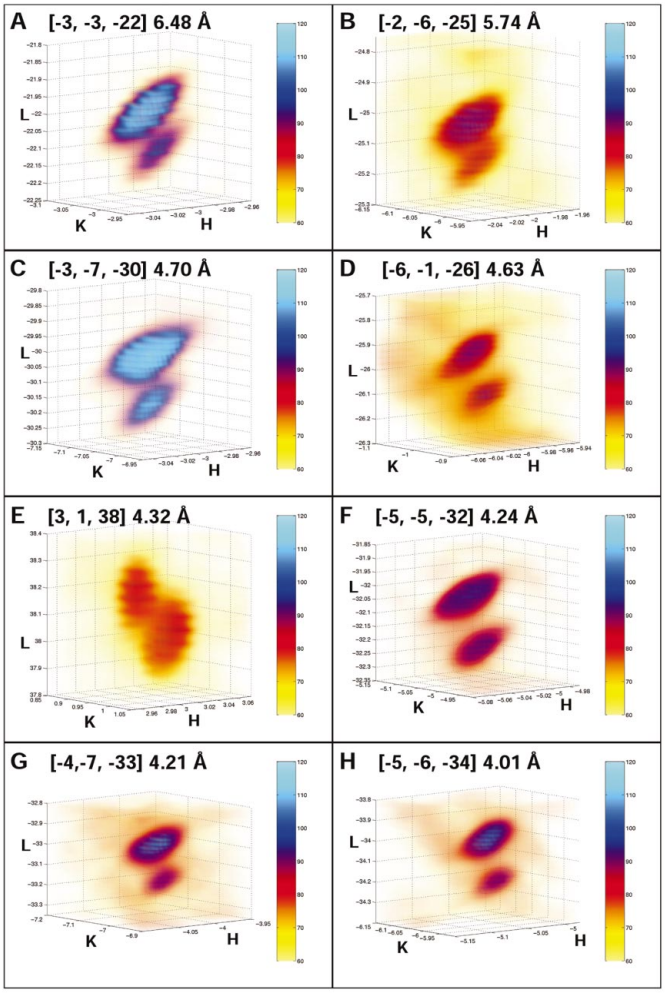

Figure 4
The three-dimensional reconstructions in reciprocal-lattice space of the eight reflections shown in Fig. 2. From left to right and top to bottom, the reflections are ordered in terms of increasing resolution. The index and resolution of each reflection are given in the upper left-hand corner of each part. The axes labels also indicate the position of the reflection index. *h* and *k* span approximately 0.2 units of reciprocal space and *l* spans approximately 0.5 units of reciprocal space. The splitting seen in the figures is similar to that seen in the original precession images for the *h*0*l* semi-crystalline state. None of these reflections is actually on the *h*0*l* plane, so a direct comparison with the precession photographs in Fig. 1 is not possible.

satellite reflections which were seen in the 0*kl* precession images (Fig. 1*b*). It is noteworthy that this phenomenon seems to occur only around a limited number of reflections in the 0*kl* plane (Fig. 1*b*) and it is not known how other higher order planes look (*e.g.* 1*kl*, 2*kl*). These preliminary experiments provide evidence that it is possible to collect diffraction data from semi-crystalline profilin:actin crystals for structure determination using fine slicing methods. Future studies will be carried out to measure all the satellite and main reflections for structure determination.

The development and application of the basic methods described here are not limited to the profilin:actin system but are generally applicable to other modulated systems. This allows investigation of naturally occurring modulation and, more excitingly, a possible new experimental technique wherein modulation can be induced to study function.

This work was based upon research conducted at the Stanford Synchrotron Radiation Laboratory, which is funded by the Department of Energy, Office of Basic Energy Sciences, USA, and was supported by NASA grants NAG8-1380 and NAG8-1825, and by the Swedish Foundation for International Cooperation in Research and Higher Education (STINT). EHS is a contractor to NASA through BAE Systems Analytical Solutions.

References

Bellamy, H. D., Snell, E. H., Lovelace, J., Pokross, M. & Borgstahl, G. E. O. (2000). *Acta Cryst.* D**56**, 986–995.
Borgstahl, G. E. O., Vahedi-Faridi, A., Lovelace, J., Bellamy, H. D. & Snell, E. H. (2001). *Acta Cryst.* D**57**, 1204–1207.
Busing, W. R. & Levy, H. A. (1967). *Acta Cryst.* **22**, 457–464.
Chik, J. K. (1996). PhD thesis, Princeton University, USA.
Chik, J. K., Lindberg, U. & Schutt, C. E. (1996). *J. Mol. Biol.* **263**, 607–623.
Daniels, P., Tamazyan, R., Kuntscher, C. A., Dressel, M., Lichtenberg, F. & van Smaalen, S. (2002). *Acta Cryst.* B**58**, 970–976.
Dehling (1927). *Z. Kristallogr.* **65**, 615–631.
Duncan, L. L., Patrick, B. O. & Brock, C. P. (2002). *Acta Cryst.* B**58**, 502–511.
Gaillard, V. B., Chapuis, G., Dusek, M. & Petricek, V. (1998). *Acta Cryst.* A**54**, 31–43.
Janssen, T., Janner, A., Looijenga-Vos, A. & Wolff, P. M. D. (1999). *Incommensurate and Commensurate Modulated Structures*, in *International Tables for Crystallography*, Vol. C, edited by A. J. C. Wilson & E. Prince. Dordrecht: Kluwer Academic Publishers.
Korekawa, M. & Jagodzinski, H. (1967). *Schweiz. Miner. Petrogr. Mitt.* **47**, 269–278.
Lovelace, J. & Borgstahl, G. E. O. (2003). *J. Appl. Cryst.* **36**, 1101–1102.
Lovelace, J., Snell, E. H., Pokross, M., Arvai, A. S., Nielsen, C., Xuong, N., Bellamy, H. D. & Borgstahl, G. E. O. (2000). *J. Appl. Cryst.* **33**, 1187–1188.
Pickersgill, R. W. (1987). *Acta Cryst.* A**43**, 502–506.
Powell, H. R. (1999). *Acta Cryst.* D**55**, 1690–1695.
Remedios, C. G. dos, Chhabra, D., Kekic, M., Dedova, I. V., Tsubakihara, M., Berry, D. A. & Nosworthy, N. J. (2003). *Physiol. Rev.* **83**, 433–473.
Rozycki, M., Schutt, C. E. & Lindberg, U. (1991). *Methods Enzymol.* **196**, 100–118.
Schutt, C. E., Kreatsoulas, C., Page, R. & Lindberg, U. (1997). *Nature Struct. Biol.* **4**, 169–172.
Schutt, C. E., Lindberg, U., Myslik, J. & Strauss, N. (1989). *J. Mol. Biol.* **209**, 735–746.
Schutt, C. E., Myslik, J. C., Rozycki, M. D., Goonesekere, N. C. & Lindberg, U. (1993). *Nature* (*London*), **365**, 810–816.
Schutt, C. E., Rozycki, M. D., Myslik, J. C. & Lindberg, U. (1995). *J. Struct. Biol.* **115**, 186–198.
Skrzypczak-Jankun, E., Bianchet, M. A., Amzel, L. M. & Funk, M. O. Jr (1996). *Acta Cryst.* D**52**, 959–965.
Snell, E. H., Judge, R. A., Crawford, L., Forsythe, E. L., Pusey, M. L., Sportiello, M., Todd, P., Bellamy, H., Lovelace, J., Cassanto, J. M. & Borgstahl, G. E. O. (2001). *Cryst. Growth Des.* **1**, 151–158.
Vahedi-Faridi, A., Lovelace, J., Bellamy, H. D., Snell, E. H. & Borgstahl, G. E. O. (2003). *Acta Cryst.* D**59**, 2169–2182.
Wonacott, A. J. (1977). *Geometry of the Rotation Method*, in *The Rotation Method in Crystallography*, edited by U. W. Arndt & A. J. Wonacott. Amsterdam: Biomedical Press.